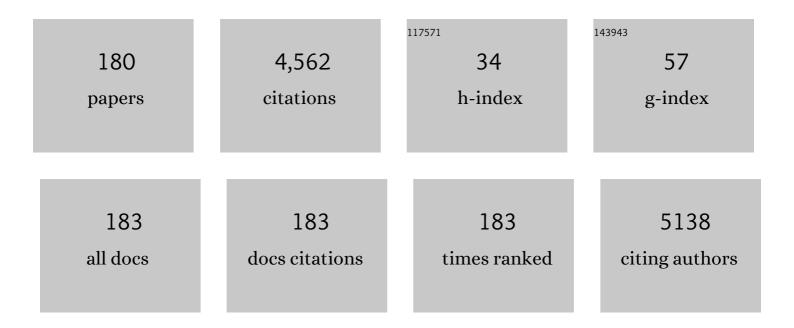
Tiju Thomas

List of Publications by Year in descending order

Source: https://exaly.com/author-pdf/1591741/publications.pdf Version: 2024-02-01



TIUL THOMAS

#	Article	IF	CITATIONS
1	Zirconium nitride catalysts surpass platinum for oxygen reduction. Nature Materials, 2020, 19, 282-286.	13.3	293
2	Multicomponent equiatomic rare earth oxides with a narrow band gap and associated praseodymium multivalency. Dalton Transactions, 2017, 46, 12167-12176.	1.6	195
3	Geopolymer for use in heavy metals adsorption, and advanced oxidative processes: A critical review. Journal of Cleaner Production, 2019, 213, 42-58.	4.6	188
4	Nickelâ€Based Transition Metal Nitride Electrocatalysts for the Oxygen Evolution Reaction. ChemSusChem, 2019, 12, 3941-3954.	3.6	150
5	Oxygen Reduction Reactions of Fe-N-C Catalysts: Current Status and the Way Forward. Electrochemical Energy Reviews, 2019, 2, 252-276.	13.1	119
6	Synthesis and application of nano-structured metal nitrides and carbides: A review. Progress in Solid State Chemistry, 2018, 50, 1-15.	3.9	104
7	Dualâ€Metal Interbonding as the Chemical Facilitator for Singleâ€Atom Dispersions. Advanced Materials, 2020, 32, e2003484.	11.1	90
8	Efficient motion retrieval in large motion databases. , 2013, , .		84
9	Recent Advances in Transition Metal Nitrideâ€Based Materials for Photocatalytic Applications. Advanced Functional Materials, 2021, 31, 2100553.	7.8	80
10	A Surfaceâ€Oxideâ€Rich Activation Layer (SOAL) on Ni ₂ Mo ₃ N for a Rapid and Durable Oxygen Evolution Reaction. Angewandte Chemie - International Edition, 2020, 59, 18036-18041.	7.2	77
11	Hierarchical N-Doped Porous Carbons for Zn–Air Batteries and Supercapacitors. Nano-Micro Letters, 2020, 12, 20.	14.4	73
12	Multivalent Cu-Doped ZnO Nanoparticles with Full Solar Spectrum Absorbance and Enhanced Photoactivity. Industrial & Engineering Chemistry Research, 2014, 53, 5895-5904.	1.8	71
13	Self-sacrificing templated formation of Co3O4/ZnCo2O4 composite hollow nanostructures for highly sensitive detecting acetone vapor. Sensors and Actuators B: Chemical, 2018, 273, 1202-1210.	4.0	69
14	Understanding the photoluminescence behaviour in nano CaZrO 3 :Eu 3+ pigments by Judd-Ofelt intensity parameters. Dyes and Pigments, 2018, 150, 306-314.	2.0	67
15	Surface Functionalized Sensors for Humidityâ€Independent Gas Detection. Angewandte Chemie - International Edition, 2021, 60, 6561-6566.	7.2	66
16	High entropy spinel metal oxide (CoCrFeMnNi)3O4 nanoparticles as a high-performance supercapacitor electrode material. Journal of Energy Storage, 2021, 42, 103004.	3.9	66
17	Comparison of experimental and calculated thermophysical properties of alumina/cupric oxide hybrid nanofluids. Journal of Molecular Liquids, 2017, 244, 469-477.	2.3	65
18	Coordination Polymer-Derived Multishelled Mixed Ni–Co Oxide Microspheres for Robust and Selective Detection of Xylene. ACS Applied Materials & Interfaces, 2018, 10, 15314-15321.	4.0	64

#	Article	IF	CITATIONS
19	Self-template derived ZnFe2O4 double-shell microspheres for chemresistive gas sensing. Sensors and Actuators B: Chemical, 2018, 265, 625-631.	4.0	64
20	What dominates heat transfer performance of hybrid nanofluid in single pass shell and tube heat exchanger?. Advanced Powder Technology, 2019, 30, 3107-3117.	2.0	63
21	Synthesis and photoluminescence properties of a novel Sr ₂ CeO ₄ :Dy ³⁺ nanophosphor with enhanced brightness by Li ⁺ co-doping. RSC Advances, 2014, 4, 38655-38662.	1.7	60
22	Ordered Mesoporous Cobalt–Nickel Nitride Prepared by Nanocasting for Oxygen Evolution Reaction Electrocatalysis. Advanced Materials Interfaces, 2019, 6, 1900960.	1.9	57
23	Auto-ignition based synthesis of Y2O3 for photo- and thermo-luminescent applications. Journal of Alloys and Compounds, 2014, 585, 129-137.	2.8	56
24	Temperature-controlled spectral tuning of full-color carbon dots and their strongly fluorescent solid-state polymer composites for light-emitting diodes. Nanoscale Advances, 2019, 1, 1413-1420.	2.2	54
25	Ruthenium Triazine Composite: A Good Match for Increasing Hydrogen Evolution Activity through Contact Electrification. Advanced Energy Materials, 2020, 10, 2000067.	10.2	52
26	Yellow-emitting carbon-dots-impregnated carboxy methyl cellulose/poly-vinyl-alcohol and chitosan: stable, freestanding, enhanced-quenching Cu ²⁺ -ions sensor. Journal of Materials Chemistry C, 2018, 6, 4508-4515.	2.7	51
27	Moss-Burstein effect in stable, cubic ZrO2: Eu+3 nanophosphors derived from rapid microwave-assisted solution-combustion technique. Materials Research Bulletin, 2018, 98, 139-147.	2.7	51
28	Charge compensation assisted enhancement of photoluminescence in combustion derived Li ⁺ co-doped cubic ZrO ₂ :Eu ³⁺ nanophosphors. Physical Chemistry Chemical Physics, 2016, 18, 29447-29457.	1.3	50
29	Mixed ternary transition metal nitrides: A comprehensive review of synthesis, electronic structure, and properties of engineering relevance. Progress in Solid State Chemistry, 2019, 53, 1-26.	3.9	50
30	Porous coral-like NiCo2O4 nanospheres with promising xylene gas sensing properties. Sensors and Actuators B: Chemical, 2018, 261, 203-209.	4.0	47
31	Nickel–Iron Nitride–Nickel Sulfide Composites for Oxygen Evolution Electrocatalysis. ACS Applied Materials & Interfaces, 2020, 12, 41464-41470.	4.0	44
32	Development of a Next-Generation Fluorescent Turn-On Sensor to Simultaneously Detect and Detoxify Mercury in Living Samples. Analytical Chemistry, 2019, 91, 3533-3538.	3.2	44
33	Ru-decorated WO3 nanosheets for efficient xylene gas sensing application. Journal of Alloys and Compounds, 2020, 826, 154196.	2.8	39
34	Machine learning-based prediction of supercapacitor performance for a novel electrode material: Cerium oxynitride. Energy Storage Materials, 2021, 40, 426-438.	9.5	35
35	Metal Oxynitrides as Promising Electrode Materials for Supercapacitor Applications. ChemElectroChem, 2019, 6, 1255-1272.	1.7	34
36	Chromium-titanium nitride as an efficient co-catalyst for photocatalytic hydrogen production. Journal of Materials Chemistry A, 2020, 8, 15774-15781.	5.2	34

#	Article	IF	CITATIONS
37	Purifying Water Containing Both Anionic and Cationic Species Using a (Zn, Cu)O, ZnO, and Cobalt Ferrite Based Multiphase Adsorbent System. Industrial & Engineering Chemistry Research, 2013, 52, 16384-16395.	1.8	33
38	Combustion synthesis approach for spectral tuning of Eu doped CaAl2O4 phosphors. Journal of Alloys and Compounds, 2014, 589, 596-603.	2.8	32
39	Structural, optical, and Raman studies of Gd doped sodium bismuth titanate. Ceramics International, 2018, 44, 12118-12124.	2.3	32
40	Engineering Co3+ cations in Co3O4 multishelled microspheres by Mn doping: The roles of Co3+ and oxygen species for sensitive xylene detection. Sensors and Actuators B: Chemical, 2020, 308, 127651.	4.0	31
41	S, N co-doped graphene quantum dots decorated TiO2 and supported with carbon for oxygen reduction reaction catalysis. International Journal of Hydrogen Energy, 2021, 46, 21549-21565.	3.8	31
42	Crystal structure classification in ABO3 perovskites via machine learning. Computational Materials Science, 2021, 188, 110191.	1.4	30
43	Luminescence enhancement in monoclinic CaAl2O4:Eu2+, Cr3+ nanophosphor by fuel-blend combustion synthesis. Chemical Engineering Journal, 2015, 267, 317-323.	6.6	29
44	Ni-Mo ternary nitrides based one-dimensional hierarchical structures for efficient hydrogen evolution. Chemical Engineering Journal, 2020, 381, 122611.	6.6	29
45	Momordica Charantia pericarp derived activated carbon with dual redox additive electrolyte for high energy density supercapacitor devices. Journal of Energy Storage, 2022, 48, 104048.	3.9	29
46	Holey Sheets of Interconnected Carbon-Coated Nickel Nitride Nanoparticles as Highly Active and Durable Oxygen Evolution Electrocatalysts. ACS Applied Energy Materials, 2018, 1, 6774-6780.	2.5	28
47	Highly Sensitive As ³⁺ Detection Using Electrodeposited Nanostructured MnO <i>_x</i> and Phase Evolution of the Active Material during Sensing. ACS Applied Materials & Interfaces, 2019, 11, 28154-28163.	4.0	27
48	Ni3N-V2O3 enables highly efficient 5-(Hydroxymethyl) furfural oxidation enabling membrane free hydrogen production. Chemical Engineering Journal, 2021, 415, 128864.	6.6	27
49	Techno-economic understanding of Indian energy-storage market: A perspective on green materials-based supercapacitor technologies. Renewable and Sustainable Energy Reviews, 2022, 161, 112412.	8.2	27
50	Ultra-small (r<2Ânm), stable (>1 year) copper oxide quantum dots with wide band gap. Superlattices and Microstructures, 2018, 113, 600-607.	1.4	26
51	Pt/WN based fuel cell type methanol sensor. Sensors and Actuators B: Chemical, 2020, 307, 127686.	4.0	26
52	Co3Mo3N—An efficient multifunctional electrocatalyst. Innovation(China), 2021, 2, 100096.	5.2	26
53	Large-scale synthesis of dual-emitting-based visualization sensing paper for humidity and ethanol detection. Sensors and Actuators B: Chemical, 2019, 282, 9-15.	4.0	25
54	Boosting Oxygen Reduction for Highâ€Efficiency H ₂ O ₂ Electrosynthesis on Oxygen oordinated CoNC Catalysts. Small, 2022, 18, e2200730.	5.2	25

Τι<mark>յ</mark>υ Τhomas

#	Article	IF	CITATIONS
55	Electric field induced short range to long range structural ordering and its influence on the Eu+3 photoluminescence in the lead-free ferroelectric Na1/2Bi1/2TiO3. Journal of Applied Physics, 2015, 117, .	1.1	24
56	Enhanced, stable, humidity-tolerant xylene sensing using ordered macroporous NiO/ZrO2 nanocomposites. Sensors and Actuators B: Chemical, 2020, 324, 128648.	4.0	24
57	Platinum decorated mesoporous titanium nitride for fuel-cell type methanol gas sensor. Sensors and Actuators B: Chemical, 2020, 308, 127713.	4.0	24
58	Nanocomposites of digestively ripened copper oxide quantum dots and graphene oxide as a binder free battery-like supercapacitor electrode material. Electrochimica Acta, 2019, 321, 134709.	2.6	23
59	Fabrication of Calotropis Gigantea fibre reinforced compression spring for light weight applications. Composites Part B: Engineering, 2019, 172, 281-289.	5.9	22
60	Metal organic framework-derived porous Fe2N nanocubes by rapid-nitridation for efficient photocatalytic hydrogen evolution. Materials Advances, 2020, 1, 1161-1167.	2.6	22
61	Surface Functionalized Sensors for Humidityâ€Independent Gas Detection. Angewandte Chemie, 2021, 133, 6635-6640.	1.6	22
62	Highly Localized C–N2 Sites for Efficient Oxygen Reduction. ACS Catalysis, 2020, 10, 9366-9375.	5.5	21
63	Synergistic Effect of Mo + Cu Codoping on the Photocatalytic Behavior of Metastable TiO ₂ Solid Solutions. Journal of Physical Chemistry C, 2014, 118, 29788-29795.	1.5	20
64	Visual and Optical Sensing of Hg ²⁺ , Cd ²⁺ , Cu ²⁺ , and Pb ²⁺ in Water and Its Beneficiation via Gettering in Nanoamalgam Form. ACS Sustainable Chemistry and Engineering, 2016, 4, 3497-3503.	3.2	20
65	Amphotericity-spectroscopy correlations in Eu doped sodium bismuth titanate (Na0.5Bi0.5TiO3). Materialia, 2019, 7, 100426.	1.3	20
66	Chromium Oxynitride as Durable Electrode Material for Symmetric Supercapacitors. Batteries and Supercaps, 2020, 3, 780-788.	2.4	20
67	Oxygen Coordination on Fe–N–C to Boost Oxygen Reduction Catalysis. Journal of Physical Chemistry Letters, 2021, 12, 517-524.	2.1	20
68	Self-Assembled, Aligned ZnO Nanorod Buffer Layers for High-Current-Density, Inverted Organic Photovoltaics. ACS Applied Materials & Interfaces, 2014, 6, 16792-16799.	4.0	19
69	Crucial Role of Donor Density in the Performance of Oxynitride Perovskite LaTiO ₂ N for Photocatalytic Water Oxidation. ChemSusChem, 2017, 10, 930-937.	3.6	19
70	Enhancement of martensite transition temperature and inverse magnetocaloric effect in Ni43Mn47Sn11 alloy with B doping. Journal of Alloys and Compounds, 2019, 795, 519-527.	2.8	19
71	Ordered mesoporous transition metal nitrides prepared through hard template nanocasting and rapid nitridation process. Journal of Alloys and Compounds, 2020, 838, 155375.	2.8	19
72	Supporting nickel on vanadium nitride for comparable hydrogen evolution performance to platinum in alkaline solution. Journal of Materials Chemistry A, 2021, 9, 19669-19674.	5.2	19

#	Article	IF	CITATIONS
73	Correlations between mechanical and photoluminescence properties in Eu doped sodium bismuth titanate. Solid State Communications, 2013, 173, 38-41.	0.9	18
74	Combining "chimie douce―and green principles for the developing world: Improving industrial viability of photocatalytic water remediation. Chemical Engineering Science, 2013, 102, 283-288.	1.9	18
75	Visible light photocatalysts (Fe, N):TiO 2 from ammonothermally processed, solvothermal self-assembly derived Fe-TiO 2 mesoporous microspheres. Materials Chemistry and Physics, 2017, 195, 259-267.	2.0	18
76	Geometric Structure and Electronic Polarization Synergistically Boost Hydrogen Evolution Kinetics in Alkaline Medium. Journal of Physical Chemistry Letters, 2020, 11, 3436-3442.	2.1	18
77	Discovery of direct band gap perovskites for light harvesting by using machine learning. Computational Materials Science, 2022, 210, 111476.	1.4	18
78	Direct band gap narrowing and light-harvesting-potential in orthorhombic In-doped-AlFeO3 perovskite: A first principles study. Journal of Alloys and Compounds, 2018, 750, 312-319.	2.8	17
79	SixC1â^'xO2 alloys: A possible route to stabilize carbon-based silica-like solids?. Solid State Communications, 2007, 144, 273-276.	0.9	16
80	Size Control and Magnetic Property Trends in Cobalt Ferrite Nanoparticles Synthesized Using an Aqueous Chemical Route. IEEE Transactions on Magnetics, 2014, 50, 1-8.	1.2	16
81	Digestive ripening and green synthesis of ultra-small (r<2nm) stable ZnO quantum dots. Ceramics International, 2014, 40, 13945-13952.	2.3	16
82	Co-precipitation strategy for engineering pH-tolerant and durable ZnO@MgO nanospheres for efficient, room-temperature, chemisorptive removal of Pb(II) from water. Journal of Environmental Chemical Engineering, 2019, 7, 103019.	3.3	16
83	Selective and Continuous Electrosynthesis of Hydrogen Peroxide on Nitrogen-doped Carbon Supported Nickel. Cell Reports Physical Science, 2020, 1, 100255.	2.8	16
84	Effect of nitridation on visible light photocatalytic behavior of microporous (Ag, Ag 2 O) co-loaded TiO 2. Microporous and Mesoporous Materials, 2017, 240, 137-144.	2.2	15
85	Indications of hard-soft-acid-base interactions governing formation of ultra-small (r < 3 nm) digestively ripened copper oxide quantum-dots. Chemical Physics Letters, 2017, 685, 84-88.	1.2	15
86	Analysis of Charge Storage Behavior in Redoxâ€electrolyte Based Batteryâ€likeâ€systems: A Case Study on Zrâ€doped Ceria. ChemistrySelect, 2020, 5, 1628-1639.	0.7	15
87	Purification and mechanical nanosizing of Eu-doped GaN. Journal of Crystal Growth, 2009, 311, 4402-4407.	0.7	14
88	Enhanced photocatalytic degradation of rhodamine B under visible light irradiation on mesoporous anatase TiO2 microspheres by codoping with W and N. Solid State Sciences, 2016, 54, 49-53.	1.5	14
89	Nanourchin ZnO@TiCN composites for Cr (VI) adsorption and thermochemical remediation. Journal of Environmental Chemical Engineering, 2018, 6, 3837-3848.	3.3	14
90	Mesoporous titanium niobium nitrides supported Pt nanoparticles for highly selective and sensitive formaldehyde sensing. Journal of Materials Chemistry A, 2021, 9, 19840-19846.	5.2	14

Τι**ju** Thomas

#	Article	IF	CITATIONS
91	Photoluminescence, thermoluminescence and EPR studies of solvothermally derived Ni2+ doped Y(OH)3 and Y2O3 multi-particle-chain microrods. Journal of Luminescence, 2014, 155, 125-134.	1.5	13
92	Enhanced visible light photocatalytic activity in N-doped edge- and corner-truncated octahedral Cu2O. Solid State Sciences, 2017, 65, 22-28.	1.5	13
93	Low defect density, high surface area LaNbON2 prepared via nitridation of La3NbO7. Materials Letters, 2017, 188, 212-214.	1.3	13
94	Critical role of surfactants in the formation of digestively-ripened, ultra-small (r<2â€ [–] nm) copper oxide quantum dots. Superlattices and Microstructures, 2018, 116, 122-130.	1.4	13
95	Investigation of magnetocaloric and mechanical properties of Ni49-xMn39Sb12Cox alloys. Journal of Alloys and Compounds, 2020, 847, 156558.	2.8	13
96	Zr substitution aided enhancement of pseudocapacitive behavior of ceria. Materials Letters, 2020, 266, 127500.	1.3	13
97	Amine coupled ordered mesoporous (Co–N) co-doped TiO ₂ : a green photocatalyst for the selective aerobic oxidation of thioether. Catalysis Science and Technology, 2017, 7, 4182-4192.	2.1	12
98	Integrating trace amounts of Pd nanoparticles into Mo ₃ N ₂ nanobelts for an improved hydrogen evolution reaction. Physical Chemistry Chemical Physics, 2022, 24, 771-777.	1.3	12
99	Soft modes at the stacking faults in SiC crystals: First-principles calculations. Physical Review B, 2008, 77, .	1.1	11
100	Chimie douce hydrogen production from Hg contaminated water, with desirable throughput, and simultaneous Hg-removal. International Journal of Hydrogen Energy, 2017, 42, 15724-15730.	3.8	11
101	Strain-induced effects in the electronic and optical properties of Na0.5Bi0.5TiO3: An ab-initio study. Materials Today Communications, 2020, 24, 101348.	0.9	11
102	Hydrogen production from human and cow urine using in situ synthesized aluminium nanoparticles. International Journal of Hydrogen Energy, 2021, 46, 27319-27329.	3.8	11
103	MOF-Derived Porous Ternary Nickel Iron Nitride Nanocube as a Functional Catalyst toward Water Splitting Hydrogen Evolution for Solar to Chemical Energy Conversion. ACS Applied Energy Materials, 2022, 5, 6155-6162.	2.5	11
104	Synthesis of Stable Al(0) Nanoparticles in Water in the form of Al(0)@Cu and Sequestration of Cu ²⁺ (aq) with Simultaneous H ₂ Production. ACS Sustainable Chemistry and Engineering, 2019, 7, 10332-10339.	3.2	10
105	Solid–Solid Separation Approach for Preparation of Carbon-Supported Cobalt Carbide Nanoparticle Catalysts for Oxygen Reduction. ACS Applied Nano Materials, 2019, 2, 3662-3670.	2.4	10
106	Correlation of micellar aggregation – complexation regimes to discern stability of micellar structure and nano-encapsulation. Journal of Colloid and Interface Science, 2019, 547, 234-244.	5.0	10
107	Experimental and Theoretical Insights of MoS 2 /Mo 3 N 2 Nanoribbonâ€Electrocatalysts for Efficient Hydrogen Evolution Reaction. ChemCatChem, 2020, 12, 122-128.	1.8	10
108	Recent Advances in Nanocasting Cobalt-Based Mesoporous Materials for Energy Storage and Conversion. Electrocatalysis, 2020, 11, 465-484.	1.5	10

#	Article	IF	CITATIONS
109	Vehicular soot for improvement of chemical stability of cement composites towards acid rain and sewage like atmospheres. Construction and Building Materials, 2020, 248, 118604.	3.2	10
110	Interface engineering of mesoporous triphasic cobalt–copper phosphides as active electrocatalysts for overall water splitting. Sustainable Energy and Fuels, 2021, 5, 1366-1373.	2.5	10
111	Amphoteric behavior of Dy3+ in Na0.5Bi0.5TiO3: Neutron diffraction and Raman studies. Ceramics International, 2021, 47, 12870-12878.	2.3	10
112	High pressure luminescence studies of europium doped GaN. Journal of Rare Earths, 2009, 27, 667-670.	2.5	9
113	Optical properties, luminescence quenching mechanism and radiation hardness of Eu-doped GaN red powder phosphor. Radiation Measurements, 2010, 45, 500-502.	0.7	9
114	Impact of solvent on the formation and optical properties of digestively ripened, ultra-small (râ€ ⁻ <â€ ⁻ 2â€ ⁻ nm) copper oxide quantum dots. Journal of Molecular Liquids, 2018, 265, 771-778.	2.3	9
115	Optimization of surface treatment in Calotropis Gigantea (CG)-fibre yarn by simple techniques and characterization of CG fibre yarn reinforced laminate. Journal of Materials Research and Technology, 2020, 9, 12187-12200.	2.6	9
116	Al–Cu core-shell nanoparticles as an alternative to noble metal plasmonics: A computational study. Materials Chemistry and Physics, 2020, 253, 123419.	2.0	9
117	Ceria for supercapacitors: Dopant prediction, and validation in a device. Applied Materials Today, 2020, 21, 100872.	2.3	9
118	Ultraâ€low Loading of Au Clusters on Nickel Nitride Efficiently Boosts Photocatalytic Hydrogen Production with Titanium Dioxide. ChemCatChem, 2020, 12, 2752-2759.	1.8	9
119	Nitridation of CoWO ₄ /CdS Nanocomposite Formed Metal Nitrides Assisting Efficiently Photocatalytic Hydrogen Evolution. ACS Omega, 2020, 5, 9969-9976.	1.6	9
120	Waste-to-wealth approach in water economy: The case of beneficiation of mercury-contaminated water in hydrogen production. International Journal of Hydrogen Energy, 2021, 46, 26677-26692.	3.8	9
121	Mesoporous Ti0.5Cr0.5N for trace H2S detection with excellent long-term stability. Journal of Hazardous Materials, 2022, 423, 127193.	6.5	9
122	Structural and Electrochemical Investigations on Nanocrystalline High Entropy Spinel Oxides for Battery‣ike Supercapacitor Applications. ChemistrySelect, 2022, 7, e202104015.	0.7	9
123	Co ₄ N–WN _{<i>x</i>} composite for efficient piezocatalytic hydrogen evolution. Dalton Transactions, 2022, 51, 7127-7134.	1.6	9
124	Methane-Sensing Performance Enhancement in Graphene Oxide/Mg:ZnO Heterostructure Devices. Journal of Electronic Materials, 2017, 46, 5485-5491.	1.0	8
125	Hole-Collecting Treated Graphene Layer and PTB7:PC ₇₁ BM-Based Bulk-Heterojunction OPV With Improved Carrier Collection and Photovoltaic Efficiency. IEEE Transactions on Electron Devices, 2018, 65, 4548-4554.	1.6	8
126	Gold Nanoclusterâ€Decorated Nickel Nitride as Stable Electrocatalyst for Oxygen Evolution Reaction in Alkaline Media. ChemElectroChem, 2019, 6, 5744-5749.	1.7	8

#	Article	IF	CITATIONS
127	Physicochemical properties of chimie douce derived, digestively ripened, ultra-small (r<2 nm) ZnO QDs. Colloids and Surfaces A: Physicochemical and Engineering Aspects, 2019, 575, 310-317.	2.3	8
128	Effective mass and optical properties of orthorhombic Al1â^'xInxFeO3 perovskite: An ab-initio study. Computational Materials Science, 2019, 159, 222-227.	1.4	8
129	Magnetism, half-metallicity and bonding in AlFeO3 and the impact of In-doping. Journal of Magnetism and Magnetic Materials, 2020, 497, 165909.	1.0	8
130	Anti-perovskite metal carbides: A new family of promising electrocatalysts for oxygen reduction in alkaline solution. Materials Research Bulletin, 2021, 133, 111014.	2.7	8
131	Scalable Drop-to-Film Condensation on a Nanostructured Hierarchical Surface for Enhanced Humidity Harvesting. ACS Applied Nano Materials, 2021, 4, 1540-1550.	2.4	8
132	Hybrid-Organic-Photodetector Containing Chemically Treated ZnMgO Layer With Promising and Reliable Detectivity, Responsivity and Low Dark Current. IEEE Transactions on Device and Materials Reliability, 2019, 19, 193-200.	1.5	7
133	Template synthesis of CoFe ₂ O ₄ extended surface microspheres for efficient water decontamination and absorption of electromagnetic waves: Twin behavior. Materials Research Express, 2019, 6, 075506.	0.8	7
134	Stability and amphotericity analysis in rhombohedral ABO3 perovskites. Materialia, 2020, 13, 100819.	1.3	7
135	Aluminium nanoparticles alloyed with other earth-abundant plasmonic metals for light trapping in thin-film a-Si solar cells. Sustainable Materials and Technologies, 2021, 28, e00250.	1.7	7
136	Chromium Oxynitride (CrON) Nanoparticles: an Unexplored Electrocatalyst for Oxygen Evolution Reaction. Electrocatalysis, 2022, 13, 62-71.	1.5	7
137	Enhanced photo-fenton and photoelectrochemical activities in nitrogen doped brownmillerite KBiFe2O5. Scientific Reports, 2022, 12, 5111.	1.6	7
138	A dimethyl disulfide gas sensor based on nanosized Pt-loaded tetrakaidecahedral α-Fe ₂ O ₃ nanocrystals. Nanotechnology, 2022, 33, 405502.	1.3	7
139	Gallium nitride powders: Mechanism of ammonothermal synthesis, ball-mill assisted rare earth doping and uniform electrophoretic deposition. Journal of Crystal Growth, 2011, 316, 90-96.	0.7	6
140	Nanorod to quantum dot conversion in ZnO dispersions with co-surfactants. RSC Advances, 2015, 5, 15154-15158.	1.7	6
141	Effect of nitrogen substitution on the structural and magnetic ordering transitions of NiCr ₂ O ₄ . RSC Advances, 2016, 6, 112140-112147.	1.7	6
142	Evidence of nano-galvanic couple formation on in-situ formed nano-aluminum amalgam surfaces for passivation-bypassed water splitting. International Journal of Hydrogen Energy, 2018, 43, 10878-10886.	3.8	6
143	Do depletant stabilized water-in-oil microemulsions have implications for nanoencapsulation?. Colloids and Surfaces A: Physicochemical and Engineering Aspects, 2019, 577, 440-448.	2.3	6
144	Flowerâ€like FeS Coated with Heteroatom (S,N)â€Doped Carbon as Highly Active and Durable Oxygen Reduction Electrocatalysts. ChemElectroChem, 2020, 7, 2433-2439.	1.7	6

Τιju Thomas

#	Article	IF	CITATIONS
145	Nitrogen, sulfur co-doped carbon coated zinc sulfide for efficient hydrogen peroxide electrosynthesis. Dalton Transactions, 2021, 50, 5416-5419.	1.6	6
146	Surface enthalpy driven size focussing trends: Predictive modelling for digestive ripening of spherical particles. Applied Surface Science, 2018, 448, 248-253.	3.1	5
147	Ordered mesoporous carbon assisted Fe–N–C for efficient oxygen reduction catalysis in both acidic and alkaline media. Nanotechnology, 2020, 31, 165708.	1.3	5
148	Semiconductor-based thermal wave crystals. ISSS Journal of Micro and Smart Systems, 2020, 9, 181-189.	1.0	5
149	FeNi ₃ –FeNi ₃ N – a high-performance catalyst for overall water splitting. Sustainable Energy and Fuels, 2020, 4, 6245-6250.	2.5	5
150	A Surfaceâ€Oxideâ€Rich Activation Layer (SOAL) on Ni 2 Mo 3 N for a Rapid and Durable Oxygen Evolution Reaction. Angewandte Chemie, 2020, 132, 18192-18197.	1.6	4
151	Iron based chalcogenide and pnictide superconductors: From discovery to chemical ways forward. Progress in Solid State Chemistry, 2020, 59, 100282.	3.9	4
152	Machine learning based a priori prediction on powder samples of sintering-driven abnormal grain growth. Computational Materials Science, 2021, 187, 110117.	1.4	4
153	Surface oxidation for enhancing the hydrogen evolution reaction of metal nitrides: a theoretical study on vanadium nitride. Materials Advances, 0, , .	2.6	4
154	Lateral Heterogeneities in ZnO Electrodeposits and Their Impact on Electrical and Optical Properties. ECS Solid State Letters, 2012, 1, P35-P37.	1.4	3
155	Size-dependent disproportionation (in ~ 2–20Ânm regime) and hybrid Bond Valence derived interatomic potentials for BaTaO2N. Applied Nanoscience (Switzerland), 2018, 8, 1379-1388.	1.6	3
156	Al-In nanoparticles and their clusters as solar spectrum plasmonic resonators. Materials Science and Engineering B: Solid-State Materials for Advanced Technology, 2019, 242, 75-82.	1.7	3
157	Multicomponent equiatomic lead strontium calcium titanate (Pb Sr Ca) Ti O3 prepared by reverse co-precipitation. Materialia, 2020, 9, 100571.	1.3	3
158	Cobalt Nanoparticles Modified Single-Walled Titanium Carbonitride Nanotube Derived from Solid-Solid Separation for Oxygen Reduction Reaction in Alkaline Solution. Electrocatalysis, 2020, 11, 579-592.	1.5	3
159	A size tunable bimetallic nickel-zinc nitride as a multi-functional co-catalyst on nitrogen doped titania boosts solar energy conversion. Dalton Transactions, 2020, 49, 4887-4895.	1.6	3
160	Multifunctional hosts of Zinc sulfide coated carbon nanotubes for lithium sulfur batteries. SN Applied Sciences, 2020, 2, 1.	1.5	3
161	Factors determining the band gap of a nanocrystalline multicomponent equimolar transition metal based high entropy oxide (Co,Cu,Mg,Ni,Zn)O. Materials Science and Engineering B: Solid-State Materials for Advanced Technology, 2022, 283, 115847.	1.7	3
162	Size Reduction and Rare Earth Doping of GaN Powders through Ball Milling. Materials Research Society Symposia Proceedings, 2009, 1202, 226.	0.1	2

#	Article	IF	CITATIONS
163	Modeling of Newtonian and non-Newtonian-based coolants for deployment in industrial length-scale shell and tube heat exchanger. International Journal of Modern Physics C, 2021, 32, 2150085.	0.8	2
164	Ionic amphiphile stabilized reverse micellar systems and their implications for nanoencapsulation. Colloids and Surfaces A: Physicochemical and Engineering Aspects, 2021, 620, 126591.	2.3	2
165	Modelling core-shell plasmonic nanoparticles as homogenous systems: An effective refractive index approach. Materialia, 2021, 19, 101183.	1.3	2
166	Organic solar cell by using vertically aligned nanostructured ZnO nanorods. , 2013, , .		1
167	Suppression of Red Luminescence in Wire Explosion Derived Eu:ZnO. Journal of Electronic Materials, 2018, 47, 1924-1931.	1.0	1
168	Size- and temperature-dependent specific heat capacity and diffusion constants of ultra-small BaTaO2N nanoparticles. Applied Nanoscience (Switzerland), 2020, 10, 767-773.	1.6	1
169	Simultaneous laser doping and annealing to form lateral p–n junction diode structure on silicon carbide films. Journal of Micromanufacturing, 0, , 251659842110162.	0.6	1
170	Carbon-Encapsulated Cobalt Phosphide Catalyst for Efficient Electrochemical Synthesis of Hydrogen Peroxide. Journal of the Electrochemical Society, 2022, 169, 024509.	1.3	1
171	Chimie douce derived Nickelt Cobalt oxynitride as electrode material for high energy density supercapacitors. Electrochimica Acta, 2022, 418, 140341.	2.6	1
172	Mo3N2/VO2 composite as electrocatalysts for hydrogen evolution reaction. Inorganic Chemistry Communication, 2022, 142, 109614.	1.8	1
173	Modelling thermochemical reversible dot-to-rod transformation in colloidal nanomaterials. Colloids and Surfaces A: Physicochemical and Engineering Aspects, 2019, 581, 123784.	2.3	0
174	Modelling Core-Shell Plasmonic Nanoparticles as Homogenous Systems: An Effective Refractive Index Approach. SSRN Electronic Journal, 0, , .	0.4	0
175	Temperature and Stability Study of All Oxynitride-Based Asymmetric Supercapacitor. ECS Meeting Abstracts, 2021, MA2021-01, 2081-2081.	0.0	0
176	Influences of Temperature on Band Energetics and Electrochemical Performance of Cerium Oxynitride in a Symmetric Aqua-Based Supercapacitor. ECS Meeting Abstracts, 2021, MA2021-01, 2080-2080.	0.0	0
177	Influence of Nitridation on Structural and Photoluminescence Behaviour of CaZrO3:Eu3+ Nanophosphors. Asian Journal of Chemistry, 2020, 32, 1515-1519.	0.1	0
178	Physical and Mathematical Modelling of Fluid and Heat Transport Phenomena in Porous Media. Engineering Materials, 2022, , 661-688.	0.3	0
179	CuO-ZnO Based Heterostructure Supported on Nitrogen-Doped Carbon for Oxygen Reduction Catalysis. ECS Meeting Abstracts, 2021, MA2021-02, 1915-1915.	0.0	0
180	Preparation of Aluminium Oxide Nanoparticles USING green synthesis. , 2021, , .		0